JOURNAL OF Materials CHEMISTRY

Intercalation of tetraazamacrocycles into molybdenum disulfide†

Rabin Bissessur,*[a] Robert I. Haines*[a] and Ralf Brüning[b]

[a]*Department of Chemistry, University of Prince Edward Island, Charlottetown, Prince Edward Island, Canada C1A 4P3. E-mail: rabissessur@upei.ca, rhaines@upei.ca*
[b]*Department of Physics, Mount Allison University, Sackville, New Brunswick, Canada E4L 1E6*

Received 22nd August 2002, Accepted 1st November 2002
First published as an Advance Article on the web 14th November 2002

A series of intercalation compounds of tetraazamacrocycles in molybdenum disulfide have been synthesized using the exfoliation and restacking properties of $LiMoS_2$. The sandwiched compounds were characterized by powder X-ray diffraction, thermogravimetric analyses, differential scanning calorimetry, and four-probe electrical conductivity measurements. The interlayer spacing of the intercalation compound was found to be dependent on the size of the macrocyclic ligand, indicating that the intercalated macrocycles are co-planar with the MoS_2 sheets.

Introduction

The synthesis and characterization of organic–inorganic nanocomposite materials achieved *via* the technique of intercalation chemistry continues to be an important field of research.[1] The inorganic components may be 3-D materials such as zeolites[2] and other inorganic network structures,[3] 2-D lamellar structures such as clays,[4] graphite,[5] graphite oxide,[6] transition metal oxides,[7] oxyhalides,[3,8] and dichalcogenides,[9] 1-D polymeric chains,[10] or zero-dimensional materials such as C_{60}.[11] On the other hand, the organic components may be small aromatic or aliphatic organic compounds,[12] polymers,[13] cryptands,[14] or crown ethers.[15] The resulting nanocomposites may exhibit properties synergistically derived from the two components, such as improved mechanical strength,[16] higher electronic conductivity,[17] increased ionic conductivity,[18] and enhanced thermal stability.[19]

Molybdenum disulfide (MoS_2) is a layered structure that has generated a great deal of interest in recent years.[20] It occurs naturally as the mineral molybdenite[21] and hence is cheap and readily available. It is already an important material with several practical applications. For instance, it is extensively used as a catalyst for the hydrodesulfurization (HDS) process, *i.e.* removal of sulfur from organosulfur compounds such as thiophene and bithiophene in fossil fuels.[22] Similar to graphite, MoS_2 is also used as a solid lubricant[23] because of its layered character. Lattice vibration frequencies have shown that the interlamellar van der Waals forces are weak.[24] Furthermore, MoS_2 may find use as a cathode material in high energy density lithium batteries.[25] The electrochemical insertion of lithium into MoS_2 is highly exothermic and the energy released can be harnessed to obtain a reversible battery system.

In spite of the tremendous importance of MoS_2 in practical applications, its intercalation chemistry using conventional redox techniques has been limited to alkali and alkaline earth metals dissolved in liquid ammonia[26] and organolithium reagents such as n-butyllithium.[27] Treatment of MoS_2 with organic molecules such as hydrazine, aniline, ammonia, or pyridine does not lead to intercalation, even if high temperatures are employed. In this respect, MoS_2 distinguishes itself from other transition metal dichalcogenides.[28] The resistance of MoS_2 toward intercalation is due to the fact that the Mo is in the +4 oxidation state and is therefore very difficult to reduce. However, MoS_2 has been shown to disperse readily into a colloidal suspension of single layers on reaction of the lithiated form of MoS_2, *i.e.* Li_xMoS_2 with water.[29] Flocculation of the layers in the presence of organic molecules,[30] clusters,[31] metal ions,[32] organometallics,[33] and polymers[13,34] results in the formation of intercalation compounds.

Recently, we utilized this exfoliation method to react single-layer MoS_2 in water with a pendant-arm tetraazamacrocycle, namely, 5,5,7,12,12,14-hexamethyl-1,4,8,11-tetraazacyclotetradecane-1-acetic acid (L^6), and intercalate it into MoS_2.[35] In this article, we report the intercalation of a series of tetraazamacrocycles to produce a family of tetraazamacrocycle–MoS_2 nanocomposites. The macrocycles L^1 to L^8 are shown in Fig. 1.

Tetraazamacrocycles are an interesting class of compounds

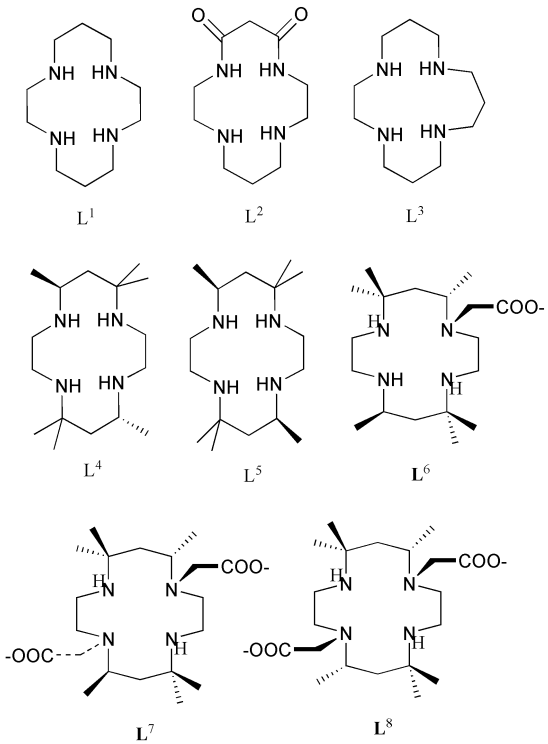

Fig. 1 Structures of macrocycles L^1–L^8.

†Electronic supplementary information (ESI) available: analytical data for L^4–L^8. See http://www.rsc.org/suppdata/jm/b2/b208237n/

 DOI: 10.1039/b208237n

in their own right. Interest in these complexes has focussed on applications to catalysis and ion selection,[36] and their use as radioimmunotherapy agents.[37] Transition metal macrocycle complexes find utility as electrocatalysts in fuel cells[38] or as catalysts for decomposition of environmentally important small molecules (NO_x, SO_x and CO_2).[39] Cobalt(III) macrocycles will bond sulfur directly to the metal,[40] and these complexes, which are also extremely stable in aggressive environments, are excellent candidates for both fundamental and applied studies of hydrodesulfurization of fossil fuels. Thus, macrocycles may provide a portal to a completely unique class of intercalation compounds, which may prove to be robust, efficient HDS catalysts.

Experimental

Synthesis of tetraazamacrocycles, L

The macrocycles L^1–L^3 were purchased from Aldrich Chemical Co. and were used without further purification. L^4 and L^5 were prepared according to the literature.[41] The acetato pendant-arm macrocycles (L^6–L^8) were prepared according to Xu and Ni.[42]

The purity of all synthesized macrocycles was confirmed by ^1H and ^{13}C NMR, FTIR, and melting point (analytical data is provided as ESI).

Preparation of Li_xMoS_2

Li_xMoS_2 was prepared by reacting MoS_2 (99%, Aldrich) with 3 equivalents of n-BuLi (2.5 M solution in hexane) in a dry box under N_2, according to eqn. 1.

$$MoS_2 + C_4H_9Li \rightarrow LiMoS_2 + 1/2C_8H_{18} \quad (1)$$

The concentration of n-BuLi was adjusted to 1 M by adding dry pentane and the reaction mixture was allowed to stir for at least 2 days at room temperature. The product was filtered off in the dry box, washed with pentane and then dried under suction. The product stoichiometry is known to be $LiMoS_2$.[13]

Synthesis of intercalation compounds

Reaction of $LiMoS_2$ with water results in the formation of single layers of MoS_2, as shown in eqn. 2. In a typical reaction, 20 mL of water was added to 200 mg of $LiMoS_2$ and the suspension sonicated for 2 h. This procedure results in complete exfoliation of the MoS_2 layers.

$$LiMoS_2 + H_2O \rightarrow (MoS_2)_{\text{single layers}} + LiOH + 1/2H_2 \quad (2)$$

In a typical experiment, an ethanolic or aqueous solution of the appropriate macrocycle (L) was added to the exfoliated MoS_2 solution and the reaction mixture allowed to stir at room temperature for two days. The mixture was then filtered and the insoluble product washed thoroughly with water and ethanol to remove LiOH and excess L. This experimental procedure leads to the formation of an intercalation compound of L into MoS_2, as shown in eqn. 3.

$$(MoS_2)_{\text{single layers}} + xL \rightarrow (L)_xMoS_2 \quad (3)$$

Instrumentation

Powder X-ray diffraction (XRD) was carried out on a diffractometer equipped with a graphite monochromator and an analyzer crystal, along with a scintillation detector. Cu-Kα radiation (λ = 1.542 Å) was utilized and the data collection was carried out at 22 °C. Samples were analyzed under vacuum with a scan range of 3 to 100°. In order to minimize scattering from materials other than those under investigation, the powdered samples were placed on a single crystal silicon substrate with the surface cut parallel to the (510) plane (supplied by The Gem Dugout, State College, PA, USA).

Thermogravimetric analyses (TGA) were performed on a Mettler Toledo Star system using a heating rate of 10 °C min^{-1}. Differential scanning calorimetry (DSC) data were obtained with a TA DSC-Q1000 apparatus using a heating rate of 5 °C min^{-1}.

Electrical conductivities were measured on pressed pellets of the samples by using the conventional four-probe technique. The diameters of the pellets were either 0.68 or 1.27 cm.

Results and discussion

Powder X-ray diffraction spectra of the products of reaction of exfoliated MoS_2 with the series of macrocycles L^1–L^8 clearly show successful intercalation of the macrocycles into the host material. In all cases, the first few (00*l*) reflections were observed, indicative of a lamellar structure. The powder diffraction pattern for $(L^7)_{0.13}MoS_2$ is shown in Fig. 2. Table 1 lists the interlayer spacings and expansions for the intercalation compounds $(L^1)MoS_2$–$(L^8)MoS_2$. The observed interlayer spacings of the intercalated compounds were between 14.49 and 10.28 Å, showing interlayer expansions in the range 8.34 to 4.13 Å relative to pristine MoS_2, which has an interlayer spacing of 6.15 Å. These expansions are consistent with monolayers of the macrocycles lying virtually co-planar with the MoS_2 sheets.

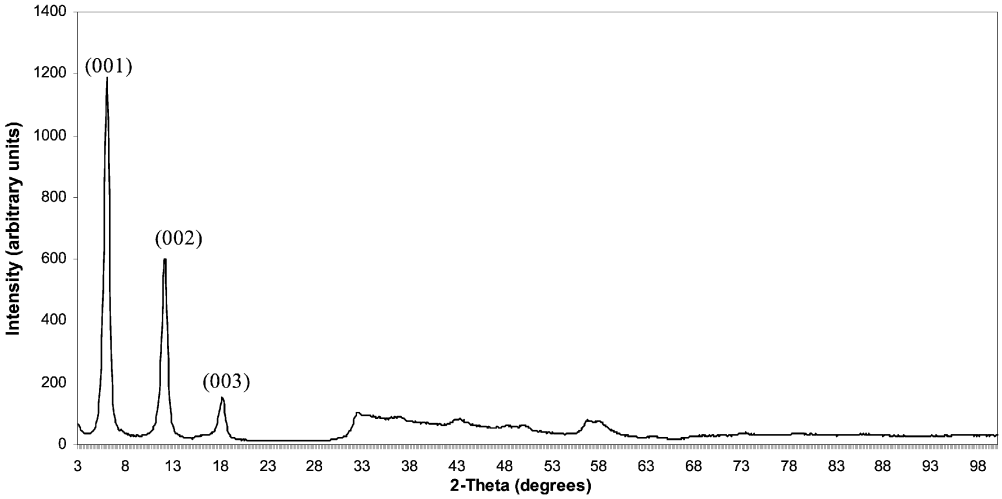

Fig. 2 Powder XRD pattern for $(L^7)_{0.13}MoS_2$.

Table 1 Interlayer spacings, interlayer expansions and estimated macrocycle thicknesses for MoS_2 phases intercalated with various tetraazamacrocycles

Macrocycle	Interlayer spacing/Å	Interlayer expansion/Å	Macrocycle dimensions	
			Thickness/Å	Cross-sectional area/Å^2
L^1	10.28	4.13	3.7	53
L^2	10.28	4.13	3.5	53
L^3	10.40	4.25	4.4	65
L^4	11.34	5.19	5.6	70
L^5	11.34	5.19	5.6	76
L^6	11.48	5.33	5.9	72
L^7	14.49	8.34	7.9	86
L^8	14.49	8.34	7.9	86

Included in Table 1 are the estimated thicknesses and cross-sectional areas of the macrocycles, determined from their geometry-optimized structures using HyperChem 6® (Hypercube Inc., Gainesville, FL, USA). It can be seen that the effective thickness of the macrocycles increases in the order L^1, $L^2 < L^3 < L^4$, $L^5 < L^6 < L^7$, L^8. L^1 and L^2 take up a chair conformation, presenting the thinnest profile. L^3, with an extra methylene group in the backbone, is a little thicker than L^1 and L^2, due to some buckling of the ring. L^4 and L^5, while having the chair conformation for their backbones, present thicker profiles due to the presence of the six methyl groups attached to the ring carbons. The thickness of L^6 is slightly greater still, due to the presence of the additional pendant acetato arm attached to the ring nitrogen. Finally, L^7 and L^8 present the greatest thickness, having two acetato pendant arms each.

From the XRD data for the last two cases, an interlayer spacing of 14.49 Å was observed, corresponding to an interlayer expansion of 8.34 Å. This value correlates very well with the calculated thickness of the macrocycles and suggests that the guest molecules are oriented within the gallery space such that they are co-planar with the disulfide sheets. Fig. 3 plots the measured interlayer expansion of the intercalation compounds *versus* the calculated macrocycle thicknesses for L^1 to L^8. Given the rather crude estimate of macrocycle thickness, there is a quite a good linear correlation between macrocycle thickness and interlayer expansion (regression slope = 0.93 ± 0.11; intercept = 0.35 ± 0.64; R^2 = 0.924), suggesting that for all compounds the macrocycles are aligned in a similar fashion, *i.e.* the intercalation compounds comprise monolayers of the guest aligned co-planar with the disulfide sheets of the host. This alignment is depicted for L^6 in Fig. 4.

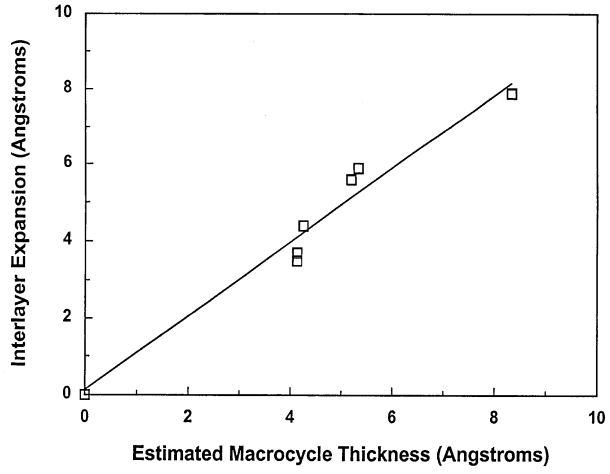

Fig. 3 Plot of measured interlayer expansion *versus* macrocycle thickness.

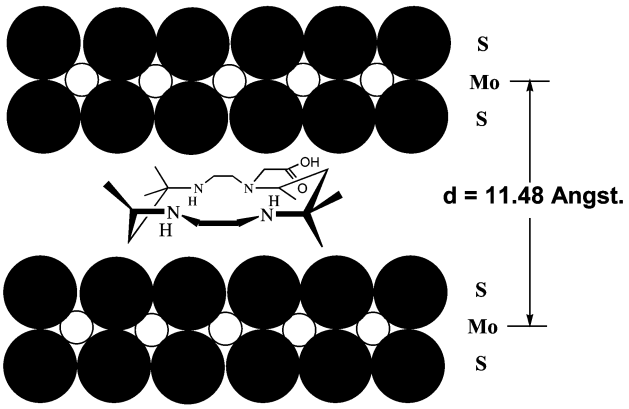

Fig. 4 Schematic illustration of the proposed structure of $(L^6)_{0.11}MoS_2$.

Similarly, intercalation compounds of L^4 and L^5 gave identical *d*-spacing, regardless of the stereochemistry of the substituents on the backbone of the macrocycles. However, the smaller interlayer spacing of 11.34 Å observed for L^4 and L^5 compared with L^7 and L^8 is consistent with the absence of pendant-arm acetato groups in the former pair. The effect of steric crowding is further demonstrated in the disulfide intercalation compounds of L^1 and L^2, which have an even smaller interlayer spacing of 10.28 Å. This is consistent with the total absence of substituents (both methyl and carboxylic acid groups) on the macrocycle.

The foregoing discussion assumes that the macrocycle loading in the intercalates represents a monolayer or less of macrocycle within each layer. From the crystallite size (below), we calculate that for a perfectly cubic crystallite, the cross-sectional area of each layer is 6400 Å^2, with 13 layers per crystallite (and therefore 12 gallery spaces). For cyclam, with an estimated rectangular cross-section of 53 Å^2, the stoichiometry of an intercalate that contains one full monolayer of macrocycle in each interlayer space would be $(cyclam)_{0.33}MoS_2$. This value stems from an estimated 1500 cyclam molecules per interlayer, and 355 MoS_2 units per layer, based on the unit cell dimensions of MoS_2.[43] Similar calculations for macrocycles L^2 to L^8 give stoichiometries of 0.38, 0.42, 0.46, 0.43, 0.51, and 0.51 macrocycles per MoS_2. Under practical conditions, perfect monolayer loading would not be achieved. Furthermore, re-stacking of layers in the intercalate is far from perfect, resulting in stepped, fragmented, and/or non-coplanar layers. It is clear that the measured stoichiometries of the intercalates correspond to loadings of less than a full monolayer of macrocycle per interlayer. That the interlayer expansions correlate well with the macrocycle thicknesses suggests that the guest molecules may act as (short) pillars, this may give rise to microporous materials.

The crystallite sizes of the intercalation compounds were estimated from their powder X-ray diffraction patterns by using the Scherrer formula.[44] A simplified version of the formula is shown in eqn. 4,

$$D = \frac{K\lambda \times 57.3}{\beta_{1/2} \cos\theta} \quad (4)$$

where D is the average crystallite size in Å, λ is the wavelength of the Cu-Kα radiation (1.542 Å), $\beta_{1/2}$ is the peak width at half-height in degrees, and θ is the position of the peak in degrees. K is a constant which depends on the shape of the crystallites. Assuming that the crystallites are perfect spheres, K is assigned a value of 0.9. The value 57.3 is the conversion factor for radians to degrees. Hence, the average crystallite size of the intercalation compounds was estimated to be *ca.* 80 Å, which may be compared with a average size of 129 Å for pristine MoS_2 used in this study. The decrease in crystallite size of

MoS_2 upon intercalation corresponds to a significant loss in crystallinity of the material, since it does not re-stack quite as well after exfoliation as in its initial state.

The intercalation compounds were characterized by thermogravimetric analysis. This technique was used to determine the thermal stabilities of the materials under both oxygen and nitrogen flow. All the materials showed good thermal stabilities under both conditions, being stable to at least 200 °C or higher in all cases (Table 2). In addition, TGA under oxygen flow was used to determine the stoichiometry of the intercalated materials. This method has been previously shown to give reliable results that agree closely with elemental analyses.[45] For example, examination of the thermogram of the intercalated phase of L^6 in MoS_2 shows that the material is stable up to 308 °C. Thereafter, a major weight loss is observed up to 450 °C, followed by the formation of MoO_3, which is stable up to 650 °C. The identity of the MoO_3 phase was confirmed by FTIR spectroscopy and XRD. The TGA data in air also show that by controlling the amount of the macrocycle in the reaction vessel, materials with varying compositions can be prepared (Table 2). However, for the macrocycles used in this research, the interlayer spacing was found to be constant irrespective of the composition of the intercalated phase. This observation suggests that we might be forming micro- or mesoporous materials and we are currently performing BET surface area measurements to measure the surface area as well as the pore size distribution; this will be the subject of a future publication.

The room temperature electrical conductivities of the intercalated phases were determined by using the conventional four-probe technique. The values obtained were in the range 0.3–0.8 S cm^{-1} (Table 3). These values are approximate since the measurements were made on pressed pellets and account must be taken of the grain boundaries in the sample. Therefore, we would expect the actual conductivity of the samples to be much higher. True conductivities could be measured using sintered pellets.[46] This is not possible, however, since sintering would cause a change in the structure of MoS_2, resulting in loss of conductivity (*vide infra*). At first sight, it may be surprising to see that the nanocomposite materials are highly conductive, since conductivity measurements at room temperature on a pressed pellet of molybdenum disulfide shows that it has a low electrical conductivity value of 5×10^{-3} S cm^{-1}. In addition, the macrocycles in isolation are discrete molecular species and are therefore non-conductors. The enhancement in electrical conductivity by a factor of 60–160 can only be explained by a structural transformation which takes place in the MoS_2 during the intercalation process. In pristine MoS_2, the molybdenum atoms are bonded to the sulfurs in a trigonal prismatic arrangement. Band structure calculations have shown that the material is a semiconductor,[47] and it has been determined to have a band gap of ~1.5 eV *via* photocurrent measurements in an electrochemical cell.[48] In this form, MoS_2 is referred to as 2H-MoS_2, or D_{3h}-MoS_2 from point group considerations (Fig. 5). Upon treatment with n-BuLi, reduction of the layers takes place, along with a structural transformation of the MoS_2 framework. The molybdenum atom is now bonded to the six sulfurs in an octahedral geometry. MoS_2 in this form is referred to as 1T-MoS_2 or O_h-MoS_2. This structural modification confers a metallic character on the disulfide, as seen in its band diagram.[49] The O_h-MoS_2 form is actually metastable and has been shown to gradually lose its conductivity upon ageing. This loss in conductivity is due to the slow conversion of the O_h form to the thermodynamically more stable D_{3h} form. The conversion is kinetically more rapid with increasing temperature. The conversion of O_h-MoS_2 to D_{3h}-MoS_2 can also be probed by differential scanning calorimetry. For instance, DSC of $(L^5)_{0.02}MoS_2$ reveals a broad exothermic peak with a peak maximum at ~200 °C (Fig. 6). This exothermic peak corresponds to the conversion of metastable O_h-MoS_2 to the thermodynamically more stable D_{3h} form. The transition was found to be irreversible and occurs with constant mass. Restacked MoS_2 has been shown to produce an exothermic peak at ~100 °C.[34] The 100 °C shift to higher temperature in $(L^5)_{0.02}MoS_2$ is due to the presence of the

Table 2 Thermal stabilities of macrocycle–MoS_2 systems in air and nitrogen. The temperature recorded is the onset of decomposition in each case. The stoichiometries were determined *via* TGA under compressed air

	Thermal stability/°C	
Intercalate	Air	N_2
$(L^1)_{0.12}MoS_2$	210	200
$(L^2)_{0.14}MoS_2$	400	200
$(L^3)_{0.12}MoS_2$	320	240
$(L^4)_{0.14}MoS_2$	200	200
$(L^4)_{0.09}MoS_2$	200	200
$(L^4)_{0.08}MoS_2$	200	200
$(L^5)_{0.10}MoS_2$	275	210
$(L^5)_{0.02}MoS_2$	275	210
$(L^6)_{0.11}MoS_2$	308	268
$(L^7)_{0.13}MoS_2$	200	200
$(L^8)_{0.07}MoS_2$	200	200

Table 3 Four-probe room temperature conductivities of macrocycle–MoS_2 intercalated phases

Intercalate	Conductivity/S cm^{-1}
$(L^1)_{0.12}MoS_2$	0.3
$(L^3)_{0.12}MoS_2$	0.6
$(L^4)_{0.14}MoS_2$	0.8
$(L^4)_{0.09}MoS_2$	0.6
$(L^4)_{0.08}MoS_2$	0.4
$(L^5)_{0.02}MoS_2$	0.7

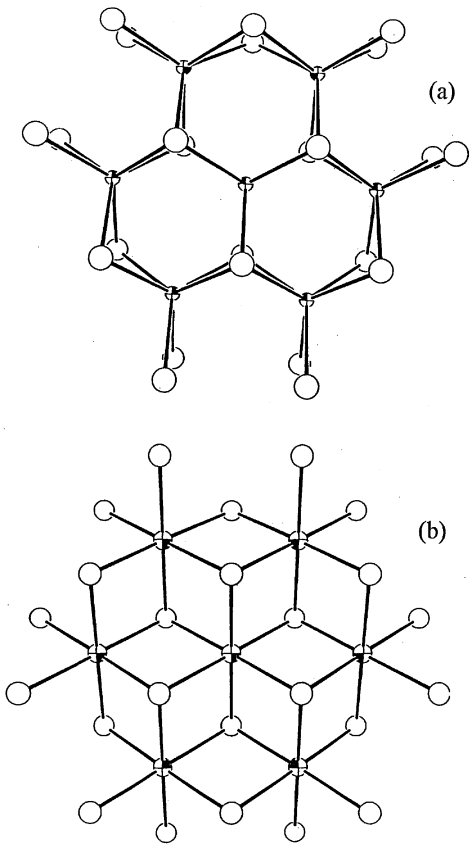

Fig. 5 Structures of (a) D_{3h}-MoS_2 and (b) O_h-MoS_2.

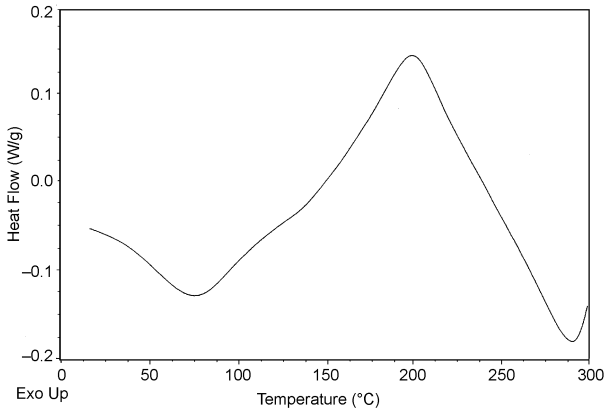

Fig. 6 DSC trace for $(L^5)_{0.02}MoS_2$.

intercalated macrocycle. In other words, the macrocycle stabilizes the O_h-MoS_2 phase. Increasing the loading to 0.10 had no effect on the conversion temperature, keeping in mind that the interlayer spacings of both $(L^5)_{0.02}MoS_2$ and $(L^5)_{0.10}MoS_2$ are the same. Therefore, the maximum in the conversion temperature seems to be dependent on the interlayer spacing of the material, regardless of the loading of the guest species.

Conclusions

The exfoliation and restacking properties of $LiMoS_2$ have proven to be very useful for producing intercalation compounds based on macrocycles. The guests are sandwiched between the host layers in a co-planar fashion, the interlayer expansions being due solely to the steric bulk of the guests. The compounds exhibit enhanced electronic conductivity, due to the alteration of the host's band structure.

We are currently extending this work to examine intercalation compounds formed between MoS_2 and transition metal macrocycle complexes that have both square-planar and octahedral geometries in order to explore the steric effects on intercalation further. We are also studying the effect of metal type and guest charge on the intercalation process, with particular emphasis on cobalt systems, given the importance of this metal in the HDS process.

Acknowledgements

Financial support from the Natural Sciences and Engineering Research Council (NSERC) and the University of Prince Edward Island Senate Committee on Research are gratefully acknowledged.

References

1 *ACS Symp. Ser.*, 1996, **622**, and references therein.
2 (*a*) T. Bein and P. Enzel, *Synth. Met.*, 1989, **29**, E163; (*b*) P. Enzel and T. Bein, *J. Phys. Chem.*, 1989, **93**, 6270.
3 C.-G. Wu, H. O. Marcy, D. C. DeGroot, J. L. Schindler, C. R. Kannewurf and M. G. Kanatzidis, *Synth. Met.*, 1991, **41**(43), 693.
4 K. E. Strawhecker and E. Manias, *Chem. Mater.*, 2000, **12**, 2943.
5 T. Zheng and J. R. Dahn, *Synth. Met.*, 1995, **73**, 1, and references therein.
6 (*a*) Y. Matsuo, K. Tahara and Y. Sugie, *Carbon*, 1997, **35**, 113; (*b*) Y. Matsuo, K. Hatase and Y. Sugie, *Chem. Mater.*, 1998, **10**, 2266; (*c*) T. Kyotani, H. Moriyama and A. Tomita, *Carbon*, 1997, **35**, 1185; (*d*) P. Liu, K. Gong, P. Xiao and M. Xiao, *J. Mater. Chem.*, 2000, **10**, 933.
7 (*a*) K. Chatakondu, M. L. H. Green, J. Qin, M. E. Thompson and P. J. Wiseman, *J. Chem. Soc., Chem. Commun.*, 1988, 223; (*b*) F. Leroux and L. F. Nazar, *Solid State Ionics*, 2000, **133**, 37.
8 I. Kargina, B. Patel and D. Richeson, *J. Chem. Res.*, 1996, (*S*)72.
9 L. Bernard, M. McKelvy and W. Glaunsinger, *Solid State Ionics*, 1985, **15**, 301.
10 (*a*) J. K. Vassiliou, R. P. Ziebarth and F. J. DiSalvo, *Chem. Mater.*, 1990, **2**, 738; (*b*) F. J. DiSalvo, *Science*, 1990, **247**, 649.
11 (*a*) K. Holczer, O. Klein, G. Gruner, J. D. Thompson, F. Diederich and R. L. Whetten, *Phys. Rev. Lett.*, 1991, **67**, 271; (*b*) K. Holczer, O. Klein, S-M. Huang, R. B. Kaner, K-J. Fu, R. L. Whetten and F. Diederich, *Science*, 1991, **252**, 1154.
12 M. S. Whittingham and A. J. Jacobson, *Intercalation Chemistry*, Materials Science Series, Academic Press, New York, 1982, and references therein.
13 R. Bissessur, J. L. Schindler, C. R. Kannewurf and M. Kanatzidis, *J. Chem. Soc., Chem. Commun.*, 1993, 1582.
14 P. Aranda, B. Casal, J. J. Fripat and E. Ruiz-Hitzky, *Langmuir*, 1994, **10**, 1207.
15 E. Ruiz-Hitzky and B. Casal, *Nature*, 1978, **7**, 596.
16 A. Okada, M. Kawasumi, A. Usuki, Y. Kojima, T. Kuraughi and O. Kamigaito, *Mater. Res. Soc. Symp. Proc.*, 1990, **171**, 45.
17 R. Bissessur, D. C. Degroot, J. L. Schindler, C. R. Kannewurf and M. G. Kanatzidis, *J. Chem. Soc., Chem. Commun.*, 1993, 687.
18 J. C. Hutchison, R. Bissessur and D. F. Shriver, *Chem. Mater.*, 1996, **8**, 1597.
19 J. Xu, Y. Hu, L. Song, Q. Wang, W. Fan, G. Liao and Z. Chen, *Polym. Degrad. Stab.*, 2001, **73**, 29.
20 E. Benavente, M. Santa Ana, F. Mendizabal and G. Gonzalez, *Coord. Chem. Rev.*, 2002, **224**, 87.
21 N. N. Greenwood andA. Earnshaw, *Chemistry of the Elements*, Pergamon Press, New York, 1984, p.1168.
22 O. Weisser and S. Landa, *Sulfided Catalysts: Their Properties and Applications*, Pergamon Press, New York, 1973.
23 P. D. Fleischauer, *Thin Solid Films*, 1987, **154**, 309.
24 T. Wieting and J. Werble, *J. Phys. Rev. B*, 1971, **3**, 4286.
25 (*a*) C. Julien, S. I. Saikh and G. A. Nazri, *Mater. Sci. Eng., B*, 1992, **15**, 73; (*b*) H. Tributsch, *Faraday Discuss. Chem. Soc.*, 1980, **70**, 190.
26 (*a*) R. Schollhorn and A. Weiss, *J. Common Met.*, 1974, **36**, 229; (*b*) R. B. Somoano, V. Hadek and A. Rembaum, *J. Chem. Phys.*, 1973, **58**, 697; (*c*) R. B. Somoano, V. Hadek, A. Rembaum, S. Samson and J. A. Woollam, *J. Chem. Phys.*, 1975, **62**, 1068; (*d*) R. B. Somoano and A. Rembaum, *Phys. Rev. Lett.*, 1971, **27**, 402.
27 M. S. Whittingham and F. R. Gamble, Jr., *Mater. Res. Bull.*, 1975, **10**, 363.
28 R. H. Friend and A. D. Yoffe, *Adv. Phys.*, 1987, **36**, 1, and references therein.
29 (*a*) M. A. Gee, R. F. Frindt, P. Joensen and S. R. Morrison, *Mater. Res. Bull.*, 1986, **21**, 543; (*b*) W. M. R. Divigalpitiya, S. Morrison and R. F. Frindt, *Thin Solid Films*, 1990, **186**, 177.
30 (*a*) W. M. R. Divigalpitiya, R. F. Frindt and S. R. Morrison, *Science*, 1989, **246**, 369; (*b*) L. Kosiodowski and A. V. Powell, *Chem. Commun.*, 1998, 2201.
31 (*a*) R. Bissessur, J. Heising, W. Hirpo and M. Kanatzidis, *Chem. Mater.*, 1996, **8**, 318; (*b*) J. Brenner, C. L. Marshall, L. Ellis, N. Tomczyk, J. Heising and M. Kanatzidis, *Chem. Mater.*, 1998, **10**, 1244.
32 M. Danot, J. L. Mansot, A. S. Golub, G. A. Protzenko, P. B. Fabritchnyi, Y. N. Novikov and J. Rouxel, *Mater. Res. Bull.*, 1994, **29**, 833.
33 A. S. Golub, I. B. Shumilova, Y. V. Zubavichus, M. Jahncke, G. Süss-Fink, M. Danot and Y. N. Novikov, *J. Mater. Chem.*, 1997, **7**, 163.
34 M. G. Kanatzidis, R. Bissessur, D. C. DeGroot, J. L Schindler and C. R. Kannewurf, *Chem. Mater.*, 1993, **5**, 595.
35 R. Bissessur, R. I. Haines, D. R. Hutching and R. Brüning, *Chem. Commun.*, 2001, 1598.
36 (*a*) J.-P. Collin and J.-P. Sauvage, *J. Chem. Soc., Chem. Commun.*, 1987, 1075; (*b*) E. Kimura, T. Koike and M. Takahashi, *J. Chem. Soc., Chem. Commun.*, 1985, 385.
37 J. P. L. Cox, K. J. Jankowski, R. Kataky, D. Parker, N. R. A. Beeley, B. A. Boyce, M. A. W. Eaton, K. Miller, A. T. Millian, A. Harrison and C. Walker, *J. Chem. Soc., Chem. Commun.*, 1989, 797.
38 B. W. Clauberg and G. Sandstede, *J. Electroanal. Chem.*, 1976, **74**, 393.
39 (*a*) J. P. Collman, M. Marrocco, P. Deisevich, C. Kooval and F. C. Anson, *J. Electroanal. Chem.*, 1979, **101**, 117; (*b*) M. M. Burley, M. R. Rhodes and T. Meyer, *Inorg. Chem.*, 1987, **26**, 1746.
40 J. Burgess, J. Fawcett, R. I. Haines, K. Singh and D. R. Russell, *Transition Met. Chem.*, 1999, **24**, 355.
41 B. E. Douglas, *Inorg. Synth.*, 1978, **18**, 10.

42 J.-D. Xu and S.-S. Ni, *Inorg. Chim. Acta*, 1986, **111**, 61.
43 F. Wypych and R. Schollhorn, *J. Chem. Soc., Chem. Commun.*, 1992, 1386.
44 P. Scherrer, *Nachr. Ges. Wiss. Gottingen, Math.-Phys.*, 1918, **Kl.2**, 96.
45 R. Bissessur, J. L. Schindler, C. Kannewurf and M. Kanatzidis, *Mol. Cryst. Liq. Cryst.*, 1994, **245**, 249–254.
46 R. I. Haines and D. G. Owen, *J. Phys. Chem. Solids*, 1986, **47**, 647.
47 M. Kertesz and R. Hoffman, *J. Am. Chem. Soc.*, 1984, **106**, 3453.
48 K. K. Kam and B. A. Parkinson, *J. Phys. Chem.*, 1982, **86**, 463.
49 (*a*) L. F. Matthesis, *Phys. Rev.*, 1973, **8**, 3179; (*b*) M. A. Py and R. R. Haering, *Can. J. Phys.*, 1983, **61**, 76.